Journal of Materials Chemistry C

Accepted Manuscript

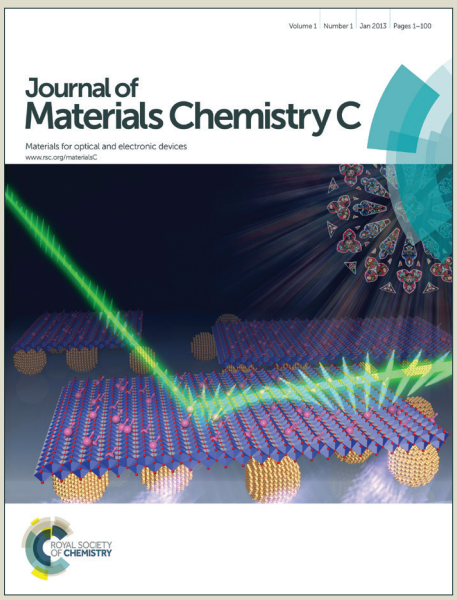

ROYAL SOCIETY OF CHEMISTRY

www.rsc.org/materialsC

Journal of Materials Chemistry C

ARTICLE

Fine-tuning gold nanorod dimensions and plasmonic properties using the Hofmeister effects†

Received 00th January 20xx,

Accepted 00th January 20xx

DOI: 10.1039/x0xx00000x

www.rsc.org/

Roger M. Pallares,[a,b] Xiaodi Su[*,b] Suo Hon Lim[b] and Nguyễn T.K. Thanh[*,c]

Gold nanorods (Au NRs) present unique optical and electronic properties that depend on their morphology. Their applications in sensing and therapeutics require easy syntheses with a precise control over their dimensions. Here, we report a method for the synthesis of highly pure and monodisperse Au NRs with fine-tuneable dimensions and longitudinal localised surface plasmon resonance by addition of Hofmeister salts into the growth medium. The control of Au NR formation relies on the double interaction between the salt-gold and salt–surfactant (cetyl trimethylammonium bromide, CTAB). With the addition of Hofmeister salts (*i.e.* $NaNO_3$, NaBr, NaCl and $NaHSO_4$) we can fine-tune the aspect ratio of Au NRs in the range of 3.3 to 4.8 with a precision of 0.1 and the longitudinal adsorption band from 777 to 960 nm. In addition, we have studied the physical changes of the CTAB micelles induced by the salts using rheology, microscopy and light-scattering techniques. We report for the first time electron microscopy imaging of the micelles under Au NR growth conditions. With the comprehensive characterization of CTAB micelle in the growth solution, this study provides a deeper understanding of the anisotropic growth of metallic crystals.

Introduction

Over the past decade nanoplasmonic field has been significantly developed due to the introduction of a variety of novel synthetic methods and biofunctionalisation strategies for new morphologies beyond sphere (*i.e.* nanorod, nanostar, nanocross, etc).[1] Anisotropic plasmonic nanoparticles have been the subject of numerous studies because of their unique optical and electronic properties, *e.g.* strong absorbance in the near-infrared,[2] higher incoupling efficiency[3] or significant increase surface-enhanced Raman spectroscopy signal.[4] Among different nanocrystals, gold nanorods have attracted great attention for their distinct nanoplasmonic properties and successful utilization in a wide range of biological applications such as photothermal therapy,[5-8] drug delivery,[9] imaging[10-13] and sensing.[14-16] One of their main features is the longitudinal localised surface plasmon resonance (L-LSPR), the light-induced coherent collective oscillation of the valence electrons through the longitudinal axis, that results in a unique and intense light absorption in a wide wavelength range.[17,18] This optical property depends highly on the aspect ratio of the rod that can be customised through the controlled synthesis.

a. *Department of Chemistry, University College London, London, WC1H 0AJ, United Kingdom*

b. *Institute of Materials Research and Engineering, A*STAR (Agency for Science, Technology and Research), 3 Research Link, Singapore, 117602*

c. *UCL Healthcare Biomagnetic and Nanomaterials Laboratories, 21 Albemarle Street, London W1S 4BS and Biophysics Group, Department of Physics and Astronomy, University College London, London, WC1E 6BT, United Kingdom.*

† *Electronic Supplementary Information (ESI) available: Summary of Hofmeister salts added into the growth solutions. Optical and morphological properties of Au NRs synthesized. Relative viscosities of all growth solutions. See DOI: 10.1039/x0xx00000x*

The most common synthesis of Au NRs is the seed-mediated method, which was initially developed by Murphy *et al.*[19] and later improved by El-Sayed *et al.*[20] This seed-mediated method is a two-step procedure. Firstly, gold seeds are obtained by the fast reduction of gold salts by $NaBH_4$. Subsequently, the obtained gold seeds are used as nucleation points for the slow reduction of the gold salts by ascorbic acid in the presence of CTAB surfactant. Interestingly, depending on the nature and structure of the seeds, different kinds of Au NRs can be obtained. Initially, Murphy *et al*. used citrate-capped penta-twinned gold nanoparticles as a seeds, which yielded twinned crystal rods with {111} faces (silverless synthesis). On the other hand, El-Sayed *et al.* synthesized the seeds in the presence of CTAB, yielding single crystal nanoparticles of 1.5 nm diameter.[21] Those seeds were later used to growth single crystal Au NRs in the presence of $AgNO_3$ (silver assisted synthesis). The exact role of CTAB in the promotion of the anisotropic growth is still unclear. At early stages, El-Sayed *et al.* suggested that the CTAB acted as a soft template.[20] However, subsequent publications indicated the CTAB adsorption in specific gold facets, favouring specific surface passivation.[22,23] Furthermore, the shape-sensitivity to CTAB impurities,[24] presence of halides[25,26] and temperature effect[27,28] were also reported. A big effort has been recently made in order to enhance the tunability and monodispersity of Au NRs. Murray *et al.* reported a synthesis with high control over the nanocrystal growth through the inclusion of aromatic additives, which changed the micellar packing of the surfactant.[29] In addition, alternative reducing agents[30,31] or different surfactants[32,33] have also been used to increase the quality of the Au NRs.

Interestingly, CTAB molecules self-assemble in spheroid shape micelles in water.[34] The addition of salts, co-surfactants or other additives can change the micellar behaviour, *e.g.* transition from sphere to rod or worm-shaped micelles.[35] In the presence of the

salts, the micellar changes are caused by the screening of the electrostatic repulsion between the polar heads of the surfactant molecules. A comparison between the effects of different anions on micellar growth showed that they follow the Hofmeister series order,[36] which is a historical classification of salt capacity to precipitate proteins in water. The protein precipitation is affected by the electrostatic forces of the ions and their capacity to affect the surrounding water structure.[37] Traditionally, the anionic order of the Hofmeister series has been considered as the following: SCN^- > ClO_4^- > I^- > ClO_3^- > NO_3^- > Br^- > Cl^- > HSO_4^- > SO_4^{2-}.

In this work, we present a new methodology to fine-tune the Au NRs while keeping the basis of the well-established seed-mediated synthesis. As mentioned earlier, the customisation of monodisperse Au NRs has been generally achieved by using alternative reducing agents, co-surfactants or organic additives. In our method, we successfully employ a fourth strategy: using the Hofmeister salts, which provide precise control over the morphology and optical properties of the crystals. Moreover, for the first time, the CTAB micelle morphology has been studied under Au NR growth conditions, yielding new insights on the anisotropic growth of the rods.

Experimental Section

Materials

The following products were used as received. Sodium nitrate ($NaNO_3$, >99%), sodium bromide (NaBr, >99%), sodium chloride (NaCl, >99%), sodium bisulfate ($NaHSO_4$, >99%), sodium thiocyanate (NaSCN, >98%), sodium perchlorate ($NaClO_4$, >98%), hydrogen tetrachloroaurate trihydrate ($HAuCl_4 \cdot 3H_2O$), silver nitrate ($AgNO_3$, 0.1 N), hydrogen chloride (HCl, 37% wt in water), L-ascorbic acid (crystalline), sodium borohydride ($NaBH_4$, 98%) were purchased from Sigma-Aldrich. Hexadecyltrimethylammonium bromide (CTAB, >98%) was purchased from Tokyo Chemical Industry.

All the water employed in the experiments was obtained with a Mili-Q Integral 5 system. All glassware was cleaned with aqua regia, rinsed extensively with water, and dried before use.

Synthesis of Au NRs

Synthesis of seeds. The reaction was performed at 22 °C. The CTAB solution (5 ml, 0.2 M) was added to a 5.0 mL solution of $HAuCl_4$ 0.5 mM. While the mixture was being vigorously stirred, 0.6 mL of ice-cold $NaBH_4$ 10 mM was added at once. The seed solution was stirred for 30 sec and was left undisturbed for 30 min. Then, the seeds were immediately used to synthesize the gold nanorods. Fresh seeds are necessary to obtain monodisperse Au NRs,[38] with most syntheses letting the seeds age between 30 min and 2 h.[22,29,32,33] In addition, CTAB solubility in water is 0.1 M at 20 ºC.[39] Thus, the shorter the aging time is, the less likely the CTAB starts precipitating.

Synthesis of rods. 250 μL of $AgNO_3$ (4 mM) were added to 5.0 mL solution of CTAB (0.1 M). The solution was kept undisturbed for 15 min, after which 5 mL of $HAuCl_4$ (1 mM), a specific volume of one of the salt solutions (Table S1) and 12 μL of HCl (37%) were added. After slow stirring, ascorbic acid (75 μL, 79 mM) was introduced into the growth solution, which lost its orange colour and yielded a colourless solution, because of the reduction of Au^{3+} to Au^{1+}. The mixture was vigorously stirred for 30 sec and 60 μL of the seed solution were added. Finally, the growth solution was vigorously stirred for 30 sec and left undisturbed for 12 h. The gold nanorods were isolated by centrifugation at 8000 rpm for 15 min followed by removal of the supernatant twice. The precipitate was re-dispersed in 10 ml of mili-Q water. It is noteworthy to mention that the stoichiometric ratio between $HAuCl_4$ and ascorbic acid is 1:1.5 in the gold reduction reaction.[40] However, this ratio presents fast reaction kinetics, which yields short[41] and not well monodisperse rods. Due to the fact that we prioritize monodispersity over yield, the 1:1.2 ratio was used with a maximum yield of 80%. Previous researchers have used the same ratio[42] or even lower.[29,32]

Characterization

Transmission electron microscopy (TEM) images were acquired with a JEM-1010 microscope operating at 100 kV. High-resolution transmission electron microscopy (HR-TEM) images were obtained with a JEM-2100 microscope operating at 200 kV. Cryo-transmission electron microscopy (cryo-TEM) imaging was performed with a Titan Krios cryo-TEM operating at 300 kV. The study of the nanoparticle and micelle morphology and size distribution was performed by analysing several TEM, HR-TEM or cryo-TEM images for every sample. The optical extinction spectra were recorded

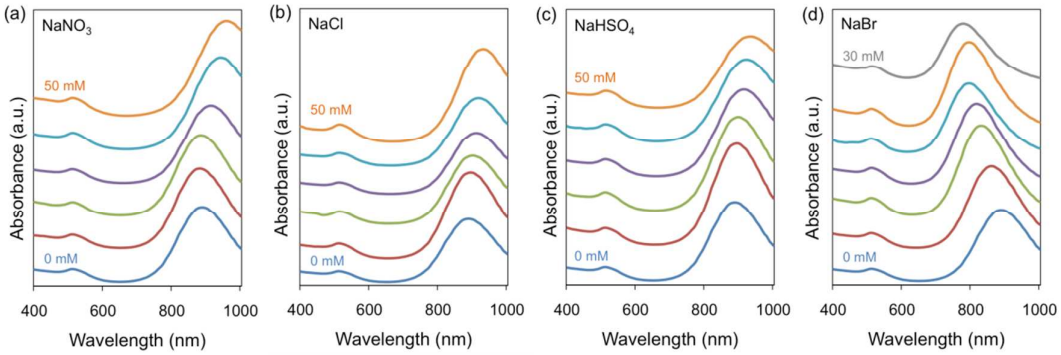

Fig. 1 Normalized extinction spectra of Au NRs grown in the presence of additional amount of Hofmeister salts. For (a), (b) and (c) the salt concentrations are 0 mM (blue), 10 mM (red), 20 mM (green), 30 mM (purple), 40 mM (turquoise) and 50 mM (orange) from bottom to top. For (d), the salt concentrations are 0 mM (blue), 5 mM (red), 10 mM (green), 15 mM (purple), 20 mM (turquoise), 25 mM (orange) and 30 mM (grey) from bottom to top. All the spectra have been offset for easier comprehension.

using a Spectramax M2/M2^{e} UV/Vis/NIR spectrophotometer. The dynamic light scattering (DLS) and zeta-potential measurements were performed with a Zetasizer Nano Z from Malvern Instruments. The X-ray diffraction (XRD) measurements were performed with D8 Discover Gadds. The viscosity data was obtained with a Cannon-Fenske viscometer.

Results and Discussion

Tuning the L-LSPR band

Even though the exact mechanism involved in the Hofmeister series is not clear, it is widely accepted that the series can be divided into different sections depending on their salting in/out effects.[43] The first group includes ions with small hydrated radii and salting out capacities (*e.g.* NH_4^+ or F^-). Following, there is a group with neutral or moderate behaviours (*e.g.* Cl^- or Na^+). Finally, the last group is composed by bigger ions with lower ionic strength, which presents salting in effect (*e.g.* SCN^- or Ca^{2+}).

In order to explore the tuning capacities of Hofmeister anions, the following six salts were studied: NaSCN, $NaClO_4$, $NaNO_3$, NaBr, NaCl and $NaHSO_4$. Na^+ was selected to be in all the salts in order to have equalised cation effect in all the experiments. All the anions were monovalent and representatives of the Hofmeister series. SCN^- and ClO_4^- present salting in ability; NO_3^-, Br^- and Cl^- are neutral members

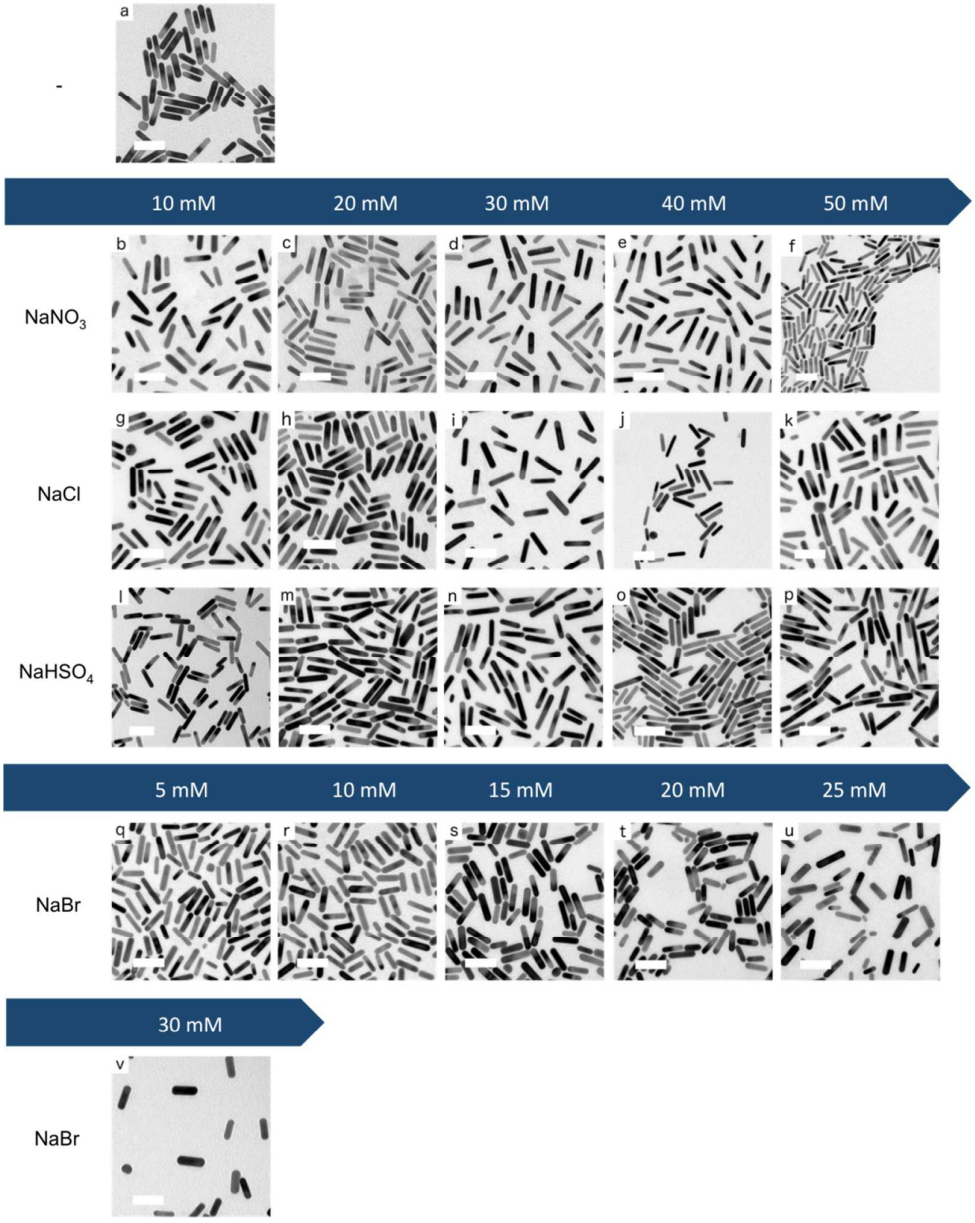

Fig. 2 TEM images of Au NRs synthesized using our seed-mediated method with different amounts of Hofmeister salts: (a) without Hofmeister salts. (b - f) with $NaNO_3$, (g - k) with NaCl and (l - p) with $NaHSO_4$ in order of increasing added concentration (10 - 50 mM). (q – v) with NaBr in order of increasing added concentration (5 – 30 mM). All scale bars are 50 nm.

of the series and HSO_4^- has salting out capacity.

As described in the Experimental section, Au NRs were synthesised using our own modified version of seed-mediated method,[20] by introducing the selected salts at different concentrations (Table S1) in the growth solution before the addition of ascorbic acid. The extinction spectra of the resulting Au NRs with $NaNO_3$, NaCl, $NaHSO_4$ and NaBr are plotted in the Fig. 1. It is important to note that the growth solution contains some Hofmeister anions from the beginning, such as bromide (from CTAB), nitride (from $AgNO_3$) and chloride (from HCl). However, their concentrations are the same in all samples, therefore their effects are equal in all the cases. The concentrations used in the text and figures are the added concentrations of Hofmeister salts.

Among six tested anion salts, SCN^- and ClO_4^- quenched the reduction reaction of gold salt and precipitated the surfactant. The colour change in the growth solution from colourless to red, which is the symbol of the Au NRs formation, was not observed. These observations were in agreement with previous studies, which showed a decrease in the reduction potential of gold ions after their conjugation with SCN^- [44] and an aggregation of the dodecyltrimethylammonium bromide (cationic surfactant with 12 aliphatic carbons instead of 16 like CTAB) induced by SCN^- and its precipitation by ClO_4^-.[45] The rest of the four salts did allow the synthesis of Au NRs and more importantly tuned the L-LSPR band either to longer or shorter wavelengths.

$NaNO_3$, NaCl and $NaHSO_4$ red-shifted the L-LSPR, with bigger changes coming from the addition of 50 mM $NaNO_3$ ($\Delta_{L\text{-}LSPR}$= 76 nm). The addition of 50 mM NaCl or 50 mM $NaHSO_4$ produced similar effects with $\Delta_{L\text{-}LSPR}$ up to 44 and 49 nm, respectively. NaBr had the biggest impact on the L-LSPR peak, *i.e.* blue-shifting it up to 107 nm from lowest to highest salt concentration. In contrast to the other salts, the maximum concentration of the added NaBr in the growth solution was 30 mM, above this amount spheroid shape particles were mainly obtained. It is worth mentioning that the low intensity of the bands around 510 nm indicates the high shape purity of the samples.

Finally, since Hofmeister series only include few representatives, the behaviour of other ions can be estimated by comparing their hydrated radii and salting in or salting out abilities with the ions contained in the series. This can be used as a tool for predicting the influence of salts in the growth of Au NRs.

Morphology and Crystalline Structure of the Au NRs

Fig. 2 shows the TEM images of the monodisperse Au NRs with small shape impurities (average below 6%) obtained by our modified El-Sayed synthesis. As expected, the variations on the aspect ratios are coherent with the shifts of the L-LSPR band induced by the salts (Table S2). Thereby, $NaNO_3$ (0-50 mM) leads to the biggest aspect ratio increases from 4.1 up to 4.8. NaCl and $NaHSO_4$ (0-50 mM) lead to similar increases in aspect ratio up to 4.7 and 4.6, respectively. On the other hand NaBr (0-30 mM) leads to a decrease of the aspect ratio from 4.1 to 3.3.

Interestingly, the increases of the aspect ratio linked to $NaNO_3$ are mainly caused by the reductions of the rod widths (from 10.6 nm to 8.8 nm), but little by rod elongations (no clear tendency of elongation), as shown in the Table S2. The increases in aspect ratios caused by NaCl and $NaHSO_4$ are due to both elongation (up to 45.6 and 45.0 nm final length, respectively, at the highest salt concentration) and width reduction (down to 9.8 nm for both salts) of the rods at the same time. On the other hand, the addition of NaBr into the growth solutions yields shorter and wider rods from 43.0 × 10.6 nm to 36.8 × 11.2 nm, resulting in lower aspect ratio crystals. The statistical significance of the different aspect ratios was studied by Welch's t-tests (Table S3) and effect size calculations (Table S4). These show that with our method the aspect ratio of the rods can be fine-tuned with a precision of 0.1 for most of the range between 3.3 and 4.8 with small effect sizes ($0.1 < d < 0.2$) but statistical significant ($p < 0.05$).

In addition, we studied the crystalline structure of Au NRs through

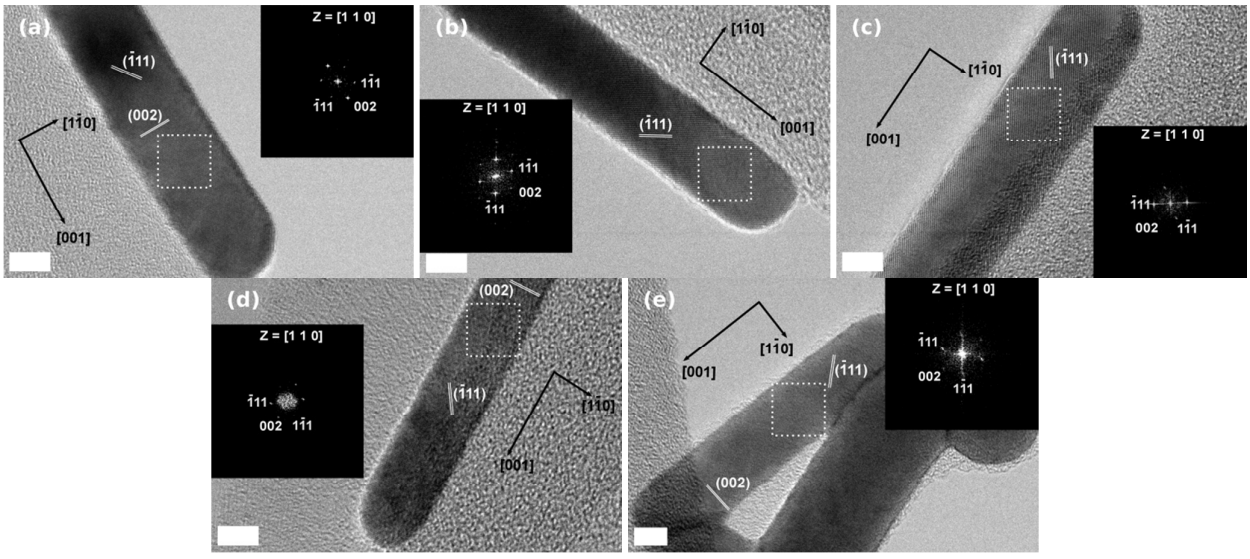

Fig. 3 HR-TEM images of Au NRs synthesized (a) without Hofmeister salts, (b) with $NaNO_3$ (50 mM), (c) with NaCl (50 mM), (d) with $NaHSO_4$ (50 mM) and (e) with NaBr (30 mM). The insets in the images are the fast Fourier transform patterns of the selected regions. All scale bars are 5 nm.

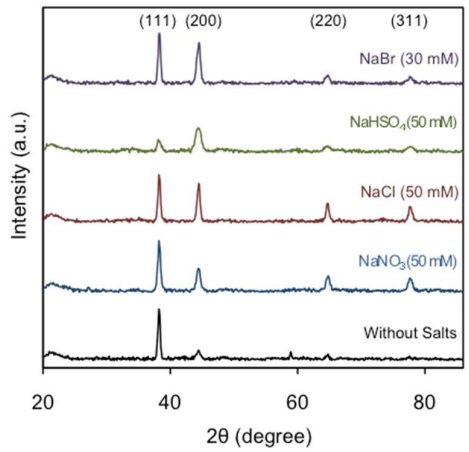

Fig. 4 XRD diffraction pattern of Au NRs obtained with and without added Hofmeister salts.

HR-TEM and XRD. The fast Fourier transform patterns of all the samples show face centered cubic (fcc) close packing, examined along [110] zone axis (Fig. 3).[46] HR-TEM data prove that the Au NRs are single-crystal. Furthermore, it is clear that the rods grow along the [001] direction. Fig. 4 shows the XRD diffraction patterns of the samples obtained with the maximum amount of Hofmeister salts. In all the cases the XRD peaks are coherent with the metallic gold where the strongest peaks are (111) and (200).[47]

Evolution of CTAB Micelles

To clarify the role of the CTAB in the synthesis of Au NRs, it is necessary to characterize the evolution of the CTAB micelles under the different growth conditions. The immiscibility between the aliphatic chain of CTAB and water induces their aggregation in cationic sphere-shaped micelles. It is well established that the electrostatic interactions between surfactant polar heads and charged species modifies the micelle zeta potential,[48] which has been suggested to play an important role on the growth of Au NRs.[28] Fig. 5a depicts the electrokinetic potential of CTAB micelles in the growth solution after the addition of different Hofmeister salt concentrations. The initial value without added Hofmeister salts is 43.5 mV and it linearly decreases with $NaNO_3$, NaCl and NaBr down to 31.1, 33.7 and 37.0 mV, respectively. Interestingly, $NaHSO_4$ is the salt that reduces the most the micellar zeta potential, down to 27.9 mV.

The interaction between the salts and the CTAB micelles also results on the screening of the electrostatic repulsion between the surfactant polar heads, which alters the surfactant packing and can trigger morphological transitions,[34] such as spherical-to-wormlike micelle transitions. The micelle morphologies have been mainly characterized by three different kinds of techniques: linear rheology, cryo-TEM and scattering based methods, as they have been deeply discussed in a recent review article.[34] Fig. 5b presents the CTAB micelle hydrodynamic diameter (D_H) in the growth solution as a function of increasing salt content measured by dynamic light scattering (DLS). The D_H increased in all the samples and was proportional to both the salt concentration and position of the anion in the Hofmeister series, suggesting that the salt triggers the micellar growth. Moreover, a larger increase of the D_H was observed for the samples with [$NaNO_3$] > 30 mM. Such kind of growth is related to the existence of interactions between the micelles, also called semi-diluted regime.

In addition to the DLS measurements, the solution viscosity was also characterised. As soon as the micelle morphology changes from sphere to rod-like or wormlike, the micelles start entangling one to each other (semi-dilute regime), subsequently the solution viscosity increases.[34] Fig. 5c plots the relative viscosity of growth solutions as a function of increasing salt content at 23 °C. Under the growth conditions, the viscosity is only affected by nitrate. Bromide, chloride and bisulphate do not show any significant effect. Interestingly, the viscosity starts increasing at $NaNO_3$ concentrations above 30 mM. Those are the same concentrations that also show semi-dilute regime by DLS.

Finally, cryo-transmission electron microscopy (cryo-TEM) studies were performed to characterise the micelle morphology in the presence of $NaNO_3$, NaCl and $NaHSO_4$ (NaBr was excluded from cryo-TEM study, because bromide anion tunes the rod aspect ratio through different mechanism, which will be described in the next section). The micelle shape has been hypothesized to play an important role on directing the Au NR growth.[20,49] Fig. 6a reveals mostly spherical CTAB micelles (97.9 %) in absence of additional Hofmeister salts, with small percentage of ellipsoidal micelles (2.1 %). Interestingly, although the spherical shape is the most common in all the samples (Fig. 6b-g), the addition of salts increases the proportion of ellipsoidal (1.5 < AR < 3) and rod-like (AR > 3) micelles

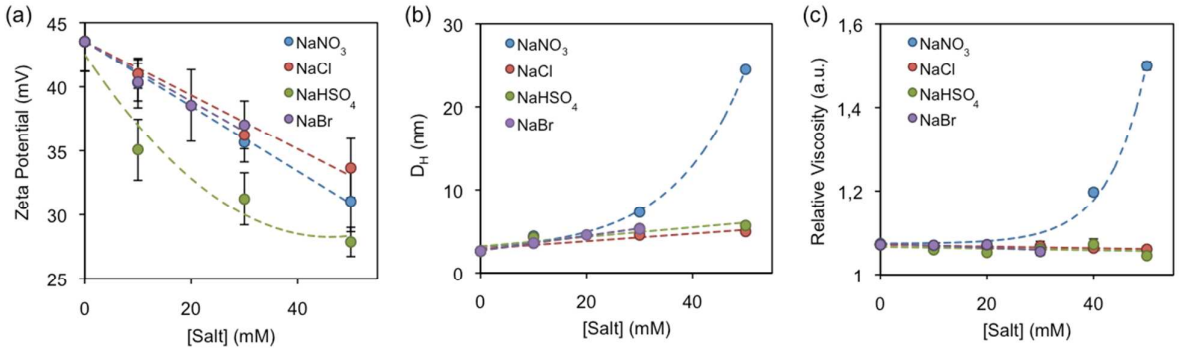

Fig. 5 (a) zeta potential, (b) hydrodynamic diameter and (c) relative viscosity of growth solutions in the presence of added Hofmeister salts.

rather than the size of all micelles (Fig. 7), and these shape transitions increases the overall micellar size observed by DLS. Nevertheless, the micelle dimensions seem to slightly increase by the addition of the salts (Table S5), however the tendency is not as clear as the increase on the number of non-spherical micelles. These results are in agreement with previously published works, which show co-existence of spherical and wormlike micelles in the same solution.[50] It is worth to mention that the only visualised solution with rod-like micelles is the one with $NaNO_3$ concentration of 50 mM. This is coherent with the semi-diluted regime observed by DLS and rheological measurements. It is important to note that the cryo-TEM images were taken from the growth solutions after the addition of the Hofmeister salts. As the growth of the Au NRs occurs, some ionic species are consumed such as Ag^+, $AuCl_4^-$ and ascorbate, which is added in the form of ascorbic acid in a second step. Therefore, the variation in their concentration might affect the CTAB micelles. Nevertheless, this seems quite unlikely since their concentrations are very low (*i.e.* the initial concentrations of silver nitrate, chloroauric acid and ascorbic acid are 0.1, 0.5 and 0.5 mM, respectively) and strong Hofmeister anions, such as nitrate, require a concentration of 10 mM to show a significant effect.

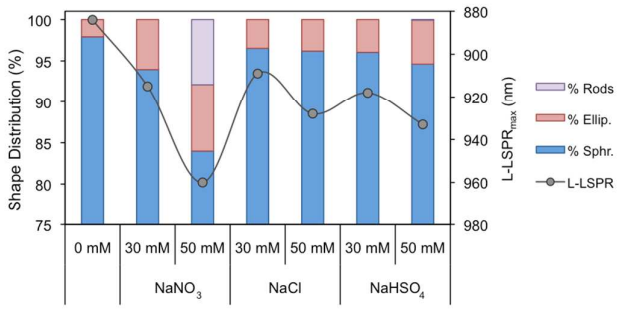

Fig. 7 Micelle shape distribution (spherical, ellipsoidal and rod-like micelle) in growth solutions at different Hofmeister salt concentrations and the L-LSPR$_{max}$ of the rods grown in those solutions.

Growth Mechanism

Despite the silver-assisted Au NR synthesis was developed over a decade ago,[20] its mechanism still very controversial and poorly understood. Currently, three main mechanisms have been proposed for the nanoparticle anisotropy: 1) the silver is under-potentially deposited at specific gold crystal faces, preventing the crystal growth at those faces;[51,52] 2) the bromide-silver complex plays a role as face-specific capping agent;[51,52] 3) CTAB micelles act as soft templates.[20,49] All three mechanisms are supported by experimental data, making it difficult to choose between the opposed theories. In a recent review,[53] Murphy *et al.* surveyed the current state-of-the-art in Au NR growth mechanism and suggests

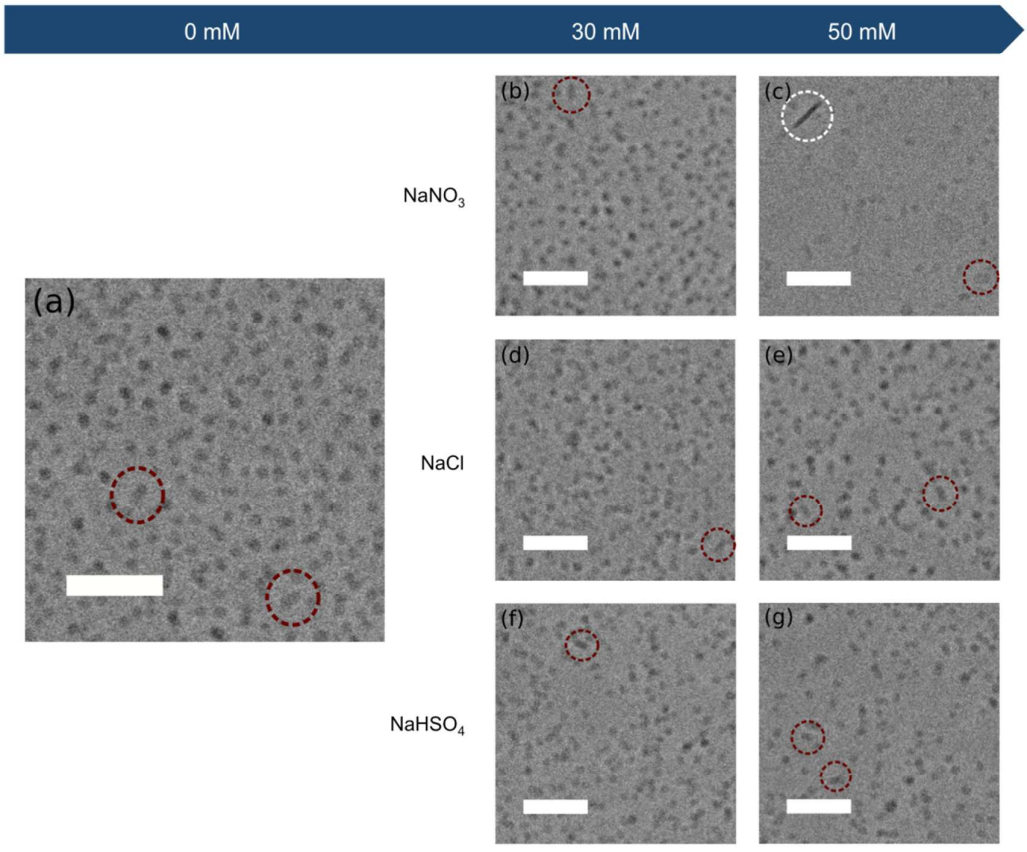

Fig. 6 Cryo-TEM images of CTAB micelles in the growth solutions with different amounts of Hofmeister salts: (a) without Hofmeister salts. (b and c) with $NaNO_3$, (d and e) with NaCl and (f and g) with $NaHSO_4$ in order of increasing added concentration (30 and 50 mM). Some ellipsoidal and rod-like micelles have been highlighted in red and white dashed circles, respectively. All scale bars are 50 nm.

that the three mechanisms may be correct to some extent, being the final mechanism a combination of all three.

Our work provides a deeper understanding of the Au NR anisotropic growth and address some of the unanswered questions described before. In this section we list the most important observations obtained from our experimental data.

First of all, it is worth mentioning that few groups have previously reported the effect of salts in the growth of Au NRs with different results than ours. Mulvaney *et al.* reported the decrease of aspect ratio after adding NaCl into the growth solution.[28] However, they were synthesizing penta-twinned Au NRs, which diverge from the single crystal Au NR in different ways, such as structure and synthetic protocol (*e.g.* low CTAB concentration, 8 mM, and absence of $AgNO_3$). On the other hand, Yong *et al.* observed increases of the aspect ratio at nitrate and chloride concentrations above 0.1 M.[49] Nevertheless, the rods obtained were highly polydisperse and presented significant shape impurities. That was probably due to the high concentration of salts in the growth solution, which may had induced wormlike micelles.[54,55]

Second, there seems to be a correlation between the decrease of CTAB electric potential and the amount of shape impurities. The addition of Hofmeister salts decreased the zeta potential of CTAB micelles to different extents and increased the shape impurities in a certain degree (Fig S1). $NaHSO_4$ induced the highest electrokinetic decrease, *i.e.* from 43.5 mV down to 27.9 mV, and yielded the highest amount of shape impurities, *i.e.* up to 13 %. NaBr induce a significant amount of spherical nanoparticles too, *i.e.* up to 9 %, however this can be account for a different mechanism that will be described later. NaCl presents a highly variable amount of shape impurities and it is difficult to get a solid conclusion. However the general impurity tendency is smaller than in the first salt. Finally, $NaNO_3$ is the salt that produces rods with higher shape purity. Even though the syntheses of penta-twinned and single crystal Au NRs follow different synthetic protocols, Mulvaney *et al.* reported a similar observation for the silverless synthesis, where the rod formation depends on *the extremely strong binding* between gold anions and cationic micelles.[28] Therefore, the decrease of the micelle zeta potential weakens the electrostatic interaction between the two spices and may drop the rod yield. In the aromatic based synthesis,[29] where organic additives are introduced to the silver-assisted synthesis, the authors hypothesized that a weaker CTAB micelle and gold precursor interaction yields shorter Au NRs. However, we did not observe such a phenomena except for the bromide, whose case will be discussed later.

Third, some works have suggested that under Au NR growth conditions,[20,49] CTAB micelles present rod-shape morphology. Thus, the Au NR anisotropy would be driven by the micelle that acts as a soft template. To the best of our knowledge, this is the first work that has visualized the CTAB micelles under Au NR synthesis conditions by cryo-electron microscopy. The surfactant micelles were mostly spherical in all the cases, with an increasing amount of ellipsoidal micelles ($1.5 < AR < 3$) with the addition of salts. Only the sample with 50 mM $NaNO_3$ presented rod-like micelles ($AR > 3$), which were significantly smaller than the resulting Au NRs, 22.8×5.0 and 42.6×8.6 nm, respectively. Therefore, the soft template seems unlikely to occur as it was proposed on those works. Nevertheless, Murray *et al.* has recently suggested that the increase of Au NR aspect ratio after the addition of organic additives is coherent with an increase of the surfactant packing parameter (p).[29] This phenomena is also observed here, where the transition of spherical micelles ($p < 1/3$)[34] to ellipsoidal and rod-like micelles ($1/3 < p < 1/2$)[34] after the addition of the salts is consistent with the shift of the AuNR L-LSPR$_{max}$ (Fig. 7). Thus, the change on the micellar behaviour, whether the surfactant molecule is directly bond to the gold, to another surface (*e.g.* under-potentially deposited silver) or in the form of a different surface-active species (*e.g.* silver-CTAB complex), seems to affect the growth of the rod.

Fourth, the samples with NaBr presented a decrease in their aspect ratio and blue-shift of the LSPR band proportional to the amount of salt, although the salt triggered the overall micellar growth. This anomalous behaviour can be explained by understanding the interaction between the bromide ions and gold. Halides are known to affect the growth of gold nanoparticles through two cooperative pathways.[56] (1) Halides anions can complex gold ion derivatives, modifying their potential and solubility and thereby altering their reduction rate.[57,58] The reduction potentials of $AuCl_2^-$, $AuBr_2^-$ and AuI_2^- are 1.154, 0.960 and 0.578 V, respectively.[59] As the lower the standard reduction potential of a complex is, the more difficult it is to be reduced by ascorbic acid. Additionally, the solubility of those complex drops in an order $AuCl_2^- > AuBr_2^- > AuI_2^-$ and the formation of less soluble compounds slows down the reaction.[60] (2) Halides can also bind to the gold surface, blocking the growth of the nanoparticle. The binding strength of the halides increase in the following order $Cl^- < Br^- < I^-$.[61] In addition, Mirkin *et al.* reported that the passivation of the gold surface by halides further disturbs the silver under-potential deposition onto gold surface.[56] This halide strong interference on the Au NR growth has been observed for iodide, where low concentrations have been reported reducing Au NRs aspect ratio and high concentrations quenching further and yielding spherical nanoparticles.[31,62] Thereby, the fact that bromide reduced the aspect ratio of the Au NRs can be explained from the gold–halide interaction point of view. Additionally, we observed a concentration threshold for bromide, *i.e.* 30 mM, like the one reported for iodide, where above that concentration the Au NRs synthesis is completely quenched and spherical particles are mainly obtained. On the contrary, chloride has less capacity to block gold deposition and it did not hinder the growth of Au NRs at the experimental concentrations. Finally, nitrate and bisulphate have been reported displaying very low affinity for gold in comparison to halides,[61,63] which explains why they did not interfere in nanoparticle growth.

Conclusions

We demonstrate that a high level of control over the rod dimensions and widely tuneable L-LSPR band can be achieved by adding small amounts of Hofmeister salts into the seed-mediated synthesis of Au NRs. The nature of the tuning depends on the double interaction between the salts with gold and the salts with surfactant micelles. Salting in ions, like thiocyanate and perchlorate, induce the surfactant precipitation and the quenching of the Au NRs formation. Neutral and salting out anions screen the electrostatic repulsion between the surfactant molecule heads, inducing changes on the micellar behaviour. When those anions

have low affinity for gold, like nitrate, bisulphate and chloride, their addition yields longer aspect ratio rods. However, anions with high affinity for gold, like bromide, reduce the gold deposition, producing shorter aspect ratio rods. Interestingly, CTAB micelles are mainly sphere-shaped in all solutions. The addition of salt increases the overall micelle size by increasing the non-spherical micelle population, although spherical shape is still the predominant one. Hence, these results provide not just a new strategy for the precise tuning of the optical properties and morphology of Au NRs, but also a deeper understanding of the anisotropic growth mechanism of the nanoparticles.

Acknowledgements

The authors are grateful to Prof. Julian Evans for providing the Cannon-Fenske viscometer. The authors thank Dr. Cristina Blanco-Andujar and Mr. Mark Turmaine for their help on the TEM measurements. The authors acknowledge Mr. Lim Poh Chong for his help on the XRD measurements. The authors thank Dr. Tran Bich Ngoc and Dr. Jian Shi for their help on cryo-TEM imaging. Roger M. Pallares thanks UCL and A*STAR for his PhD studentship. Su X thanks A*STAR JCO funding 14302FG096. Nguyen T. K. Thanh thanks the Royal Society for her Royal Society University Research Fellowship.

Notes and references

1 A. Guerrero-Martínez, M. Grzelczak and L. M. Liz-Marzán, *ACS nano,* 2012, **6**, 3655-3662.
2 F. Hao, C. L. Nehl, J. H. Hafner and P. Nordlander, *Nano Letters,* 2007, **7**, 729-732.
3 S. Nauert, A. Paul, Y. R. Zhen, D. Solis Jr, L. Vigderman, W. S. Chang, E. R. Zubarev, P. Nordlander and S. Link, *ACS Nano,* 2013, **8**, 572-580.
4 L. Vigderman and E. R. Zubarev, *Langmuir*, 2012, **28**, 9034-9040.
5 X. Huang, P. K. Jain, I. H. El-Sayed and M. A. El-Sayed, *Lasers in medical science,* 2008, **23**, 217-228.
6 L. C. Kennedy, L. R. Bickford, N. A. Lewinski, A. J. Coughlin, Y. Hu, E. S. Day and R. A. Drezek, *Small,* 2011, **7**, 169-183.
7 X. Huang, S. Neretina and M. A. El□Sayed, *Advanced Materials,* 2009, **21**, 4880-4910.
8 T. B. Huff, L. Tong, Y. Zhao, M. N. Hansen, J. X. Cheng and A.Wei, *Future Medicine,* 2007, **2**, 125-132.
9 A. M. Alkilany, L. B. Thompson, S. P. Boulos, P. N. Sisco and C. J. Murphy, *Advanced drug delivery reviews,* 2012, **64**, 190-199.
10 P. K. Jain, X. Huang, I. H. El-Sayed and M. A. El-Sayed, *Accounts of Chemical Research,* 2008, **41**, 1578-1586.
11 C. Kim, C. Favazza and L. V. Wang, *Chemical reviews,* 2010, **110**, 2756-2782.
12 A. S. Stender, K. Marchuk, C. Liu, S. Sander, M. W. Meyer, E. A. Smith and N. Fang, *Chemical reviews,* 2013, **113**, 2469-2527.
13 H. Wang, T. B. Huff, D. A. Zweifel, W. He, P. S. Low, A. Wei and J. X. Cheng, *Proceedings of the National Academy of Sciences of the United States of America,* 2005, **102**, 15752-15756.
14 L. Vigderman, B. P. Khanal and E. R. Zubarev, *Advanced Materials,* 2012, **24**, 4811-4841.
15 R. M. Pallares, S. L. Kong, T. H. Ru, N. T. Thanh, Y. Lu and X. Su, *Chemical Communications*, 2015, **51**, 14524-14527.
16 M. E. Stewart, C. R. Anderton, L. B. Thompson, J. Maria, S. K. Gray, J. A. Rogers and R. G. Nuzzo, *Chemical reviews,* 2008, **108**, 494-521.
17 S. K. Ghosh and T. Pal, *Chemical Reviews,* 2007, **107**, 4797-4862.
18 K. A. Willets and R. P. Van Duyne, *Annu. Rev. Phys. Chem.,* 2007, **58**, 267-297.
19 N. R. Jana, L. Gearheart and C. J. Murphy, *J. Phys. Chem. B,* 2001, **105**, 4065-4067.
20 B. Nikoobakht and M. A. El-Sayed, *Chemistry of Materials,* 2003, **15**, 1957-1962.
21 M. Liu and P. Guyot-Sionnest, *J. Phys. Chem. B*, 2005, 109, 22192-22200.
22 N. R. Jana, L. Gearheart and C. J. Murphy, *Advanced Materials,* 2001, **13**, 1389-1393.
23 J. Pérez-Juste, I. Pastoriza-Santos, L. M. Liz-Marzán and P. Mulvaney, *Coordination Chemistry Reviews,* 2005, **249**, 1870-1901.
24 D. K. Smith and B. A. Korgel, *Langmuir,* 2008, **24**, 644-649.
25 S. E. Lohse, N. D. Burrows, L. Scarabelli, L. M. Liz-Marzán and C. J. Murphy, *Chemistry of Materials,* 2013, **26**, 34-43.
26 S. Si, C. Leduc, M. H. Delville and B. Lounis, *ChemPhysChem,* 2012*,* **13**, 193-202.
27 K. C. Ng and W. Cheng, *Nanotechnology*, 2012, **23**, 105602-105612.
28 J. Pérez□Juste, L. M. Liz□Marzan, S. Carnie, D. Y. Chan and P. Mulvaney, *Advanced Functional Materials,* 2004, **14**, 571-579.
29 X. Ye, L. Jin, H. Caglayan, J. Chen, G. Xing, C. Zheng and C. B. Murray, *ACS nano,* 2012, **6**, 2804-2817.
30 L. Vigderman and E. R. Zubarev, *Chemistry of Materials,* 2013, **25**, 1450-1457.
31 L. Zhang, K. Xia, Z. Lu, G. Li, J. Chen, Y. Deng and N. He, *Chemistry of Materials,* 2014, **26**, 1794-1798.
32 X. Ye, Y. Gao, J. Chen, D. C. Reifsnyder, C. Zheng and C. B. Murray, *Nano letters,* 2013, **13**, 2163-2171.
33 X. Ye, C. Zheng, J. Chen, Y. Gao and C. B. Murray, *Nano letters,* 2013, **13**, 765-771.
34 C. A. Dreiss, *Soft Matter,* 2007, **3**, 956-970.
35 S. Kumar, A. Z. Naqvi and Kabir-ud-Din, *Langmuir,* 2000, **16**, 5252-5256.
36 L. Abezgauz, K. Kuperkar, P. A. Hassan, O. Ramon, P. Bahadur and D. Danino, *Journal of colloid and interface science,* 2010, **342**, 83-92.
37 M. G. Cacace, E. M. Landau and J. J. Ramsden, *Quarterly reviews of biophysics,* 1997, **30**, 241-277.
38 X. C. Jiang and M. P. Pileni, *Colloids and Surfaces A: Physicochemical and Engineering Aspects*, 2005, **295**, 228-232.
39 T. Zhang, A. Jiang, J. H. Harrison and S. Chen, *Journal of Chemical Technology and Biotechnology*, 2012, **87**, 1098-1103.
40 O. R. Miranda, N. R. Dollahon and T. S. Ahmadi, *Crystal growth & design*, 2006, **6**, 2747-2753.
41 T. K. Sau and C. J. Murphy, *Langmuir*, 2004, **20**, 6414-6420.
42 R. C. Wadams, L. Fabris, R. A. Vaia and K. Park, *Chemistry of Materials* 2013, **25**, 4772-4780.
43 Y. Zhang and P. S. Cremer, *Current opinion in chemical biology,* 2006, **10**, 658-663.
44 M. J. Nicol, C. A. Fleming, R. L. Paul, The Chemistry of Gold Extraction, in The Extractive Metallurgy of Gold, *ed. G. G. Stanley*, South African Institute of Mining and Metallurgy, Johannesburg, 1987, 831-905.
45 A. L. Underwood and E. W. Anacker, *Journal of colloid and interface science,* 1987, **117**, 242-250.
46 A. B. Shah, S. T. Sivapalan, B. M. DeVetter, T. K. Yang, J. Wen, R. Bhargava, C. J. Murphy and J. M. Zuo, *Nano letters,* 2013, **13**, 1840-1846.
47 H. W. Wang, C. F. Shieh, H. Y. Chen, W. C. Shiu, B. Russo and G. Z. Cao, *Nanotechnology*, 2006, **17,** 2689-2694.

48 R. Kumar and S. R. Raghavan, *Soft Matter,* 2009, **5**, 797-803.
49 K. T. Yong, Y. Sahoo, M. T. Swihart, P. M. Schneeberger and P. N. Prasad, *Topics in Catalysis,* 2008, **47**, 49-60.
50 K. Kuperkar, L. Abezgauz, K. Prasad and P. Bahadur, Journal of Surfactants and Detergents, **13**, 2010, 293-303.
51 P. K. Jain, X. Huang, I. H. El-Sayed and Mostafa A. El-Sayed, *Accounts of Chemical Research,* 2008, **41**, 1578-1586.
52 E. C. Dreaden, A. M. Alkilany, X. Huang, C. J. Murphy and M. A. El-Sayed, *Chemical Society Reviews*, 2012, **41**, 2740-2779.
53 S. E. Lohse and C. J. Murphy, *Chemistry of Materials,* 2013, **25**, 1250-1261.
54 M. E. Helgeson, T. K. Hodgdon, E. W. Kaler and N. J. Wagner, *Journal of colloid and interface science,* 2010, **349**, 1-12.
55 K. Kuperkar, L. Abezgauz, D. Danino, G. Verma, P. A. Hassan, V. K. Aswal and P. Bahadur, *Journal of colloid and interface science,* 2008, **323**, 403-409.
56 M. R. Langille, M. L. Personick, J. Zhang and C. A. Mirkin, *Journal of the American Chemical Society,* 2012, **134**, 14542-14554.
57 J. Rodríguez-Fernández, J. Pérez-Juste, P. Mulvaney and L. M. Liz-Marzán, *The Journal of Physical Chemistry B,* 2005, **109**, 14257-14261.
58 M. Eguchi, D. Mitsui, H. L. Wu, R. Sato and T. Teranishi, *Langmuir,* 2012, **28**, 9021-9026.
59 A. J. Bard, R. Parsons and J. Jordan, Standard Potentials in Aqueous Solution; *Marcel Dekker*: New York, 1985.
60 L. Brown and T. Holme, Chemistry for Engineering Students; *Brooks/Cole*: Belmont, 2011.
61 O. M. Magnussen, *Chemical Reviews,* 2002, **102**, 679-726.
62 D. K. Smith, N. R. Miller and B. A. Korgel, *Langmuir,* 2009, **25**, 9518-9524.
63 J. P. Sylvestre, S. Poulin, A. V. Kabashin, E. Sacher, M. Meunier and J. H. Luong, *The Journal of Physical Chemistry B,* 2004, **108**, 16864-16869.